Light Metals 2012 *Edited by: Carlos E. Suarez*
TMS (The Minerals, Metals & Materials Society), 2012

CHARACTERIZATION OF THE COMPRESSIVE BEHAVIOUR OF AN AL FOAM BY X-RAY COMPUTERIZED TOMOGRAPHY

G. Costanza[1], F. Mantineo[2], S. Missori[1], A. Sili[2], M.E. Tata[1]
[1]Dipartimento Ingegneria Meccanica - Università di Roma "Tor Vergata" - Via del Politecnico, 1 – 00133 Roma Italy
[2]Dipartimento Chimica Industriale e Ingegneria dei Materiali - Università di Messina – Contrada di Dio - 98166 Messina Italy

Keywords: Al Foam, X-Ray tomography, Compressive behaviour

Abstract

Al metal foams manufactured by the powder-method have been investigated. Compression tests were performed on the same sample at increasing deformation steps: at each stage the sample was observed by X-ray computerized tomography. A geometric evaluation of porosity on many sections was performed by calculating, for each pore, its area, equivalent diameter, perimeter and circularity.

Introduction

Metal foams are attractive for light metals applications and energy absorption due to their cellular microstructure. In the last years the attention of many researchers has been focused on the characterisation and modelling of Al foam [1, 2]. Recent studies showed that the cells structure has a substantial effect on compression behaviour [3, 4], since the amount of the absorbed energy is directly related to the way the cells structure collapses [5, 6]. Idealized microstructures having a simple geometry are developed in literature, combining 2D metallographic images and statistic theory [7], neglecting the geometrical complexity of the real 3D microstructure. The compressive properties, such as the elastic modulus and plastic plateau stress of the cellular material are important parameters for the mechanical design of the component under compression. These mechanical properties are strictly connected to the microstructure, porosity size, dimension and shape, wall thickness fractured cell walls and so on.
In this work an Al foam with closed cells, produced starting from powder with the addiction of TiH_2 as blowing agent, was considered. Its behaviour under compression was investigated by X-ray computerized tomography. Tomographic analysis were performed at increasing steps of compression in order to observe the evolution during deformation of the morphology of the cells and their final collapse.

Materials and methods

Foam production
Al foam samples have been manufactured and characterized in our laboratory. Production by the powder-method has been reported in details in a previous paper [8]. In our study it has been employed TiH_2 (average diameter 5 μm) as blowing agent and SiC (37 μm) as stabilizing agent for Al powder (45 μm). The composition is: 0.4 (wt%) for TiH_2, 2.8 SiC (wt%) and Al (to balance).
After mixing for 10 minutes with a specific device, the mixture has been successively compacted by a hydraulic press (load 12 ton) into a mould to obtain a precursor (diameter 15 mm, height 8 mm) ready to be foamed into the furnace. 700 °C is the temperature of the furnace, 300 seconds is the time required for foaming in a cylindrical mould. This combination of temperature and time permanence in the furnace has been chosen because shows a good compromise for the viscosity of the melt and the drainage.

Compression test
Compression tests were carried out on a cylindrical sample (ϕ = 15 mm, h = 24 mm), submitted to a preliminary compression to make flat the two base surfaces. The parallelism between the two platens was adjusted through the examination of the contact surface between them before the compression test. The tests were performed on the same sample with three steps of increasing compression deformation: at each step the sample was loaded, unloaded and observed by computerized tomography.

Tomographic observations
The cells morphology evolution during compression was investigated by means of a variable focus X-ray computerized tomograph (CT). Measurements by CT allows to perform sample volumetric models with high point densities (several million points) and even information of commonly not accessible inner parts. The object to be inspected is rotated inside the radiation cone beam produced by X-ray source. The intensity distribution of the radiation after passing the work-piece is measured by means of a flat panel detector and digitally stored. After recording all the projection data, during a full rotation of the sample, the volume data can be obtained by computerized 3D reconstruction. Figure 1 shows the set-up of a cone-beam and the scheme of the recording process respectively.

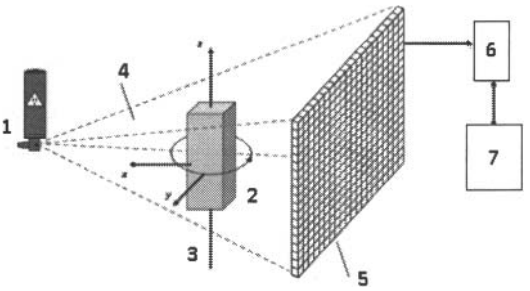

Fig. 1 Setup of a CT system: 1) X-ray source, 2) sample, 3) sample rotation axis, 4) X-ray cone beam, 5) flat panel detector, 6) data acquisition device, 7) image reconstruction device.

Our measurements were performed by a CT equipment, with variable focal spot size, Cu X-ray tube and maximum accelerating voltage of 225 kV. By changing operative parameters (sample dimension, focal spot size and distance between X-ray source and sample), the observation of samples with different X-ray absorption properties, such as bulk object or foams, can be optimised in the range micro/macrofocus working conditions as

concern as X-ray penetrating depth and spatial resolution (up to ~ 30 μm resolution for ~ 40 mm object size).

Image analysis

From the reconstructed volume, resulting by CT measurements, 3D images and 2D section of the observed sample were obtained. The 2D sections were processed to enhance contrast and brightness and then transformed into their negative images. On such images a threshold value was defined for classifying each pixel as belonging to wall or empty zone of the cell. A geometric evaluation of porosity was performed by calculating for each cell its area, equivalent diameter, perimeter and circularity. The cell area A is calculated from the number of pixel counted in a single cell.

The equivalent diameter is given by the following relationship:

$$D_{eq} = \sqrt{4A/\pi} \quad (1)$$

The average perimeter is calculated by the Crofton relationship:

$$P = \pi [P_{0°} + P_{45°} + P_{90°} + P_{135°}] / 4 \quad (2)$$

where $P_{0°} + P_{45°} + P_{90°} + P_{135°}$ are perimeters measured on four projections of the cell.

The circularity is given by the following relationship:

$$C = 4 \pi A / P^2 \quad (3)$$

The geometric evaluation of porosity during compression test was performed on representative sections of the samples, recorded at each compression step.

Results and discussion

The loading-unloading curves of each compression step were assembled obtaining the compression diagram in fig. 2, that agrees to the behaviour of an Al foam during a monotonic compression test.

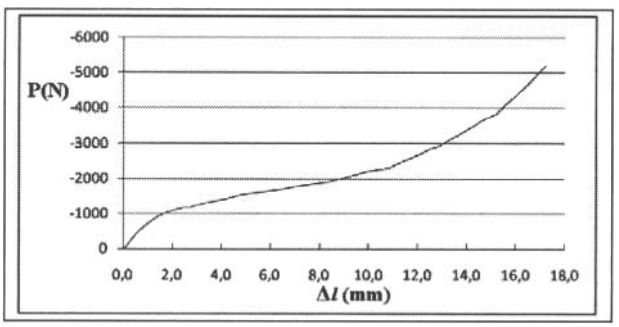

Fig. 2 Compression diagram: load P (N) vs. sample reduction length Δl (mm).

The diagram in fig. 2 is characterized by an initial region of linear elasticity and is followed by a roughly constant plateau stress (plastic deformation) up to strain of the order of 50-60%. Beyond this value the stress increases sharply due to the cells collapse in the full sample.

The geometrical data of the sample (15 mm starting diameter), measured at each compression step, are given in table 1.

Table 1 – Sample geometric data at each compression step

	Starting height (mm)	Final height (mm)	Final diameter (mm)
precompr. sample (step 0)	25,7	23,33	15,35
compression (step 1)	20,96	20,16	15,55
compression (step 2)	17,84	15,55	16,19
compression (step 3)	13,28	11,04	17,14

Figure 3 shows the rendering of the reconstructed volumes of the sample, observed by CT after each compression step.

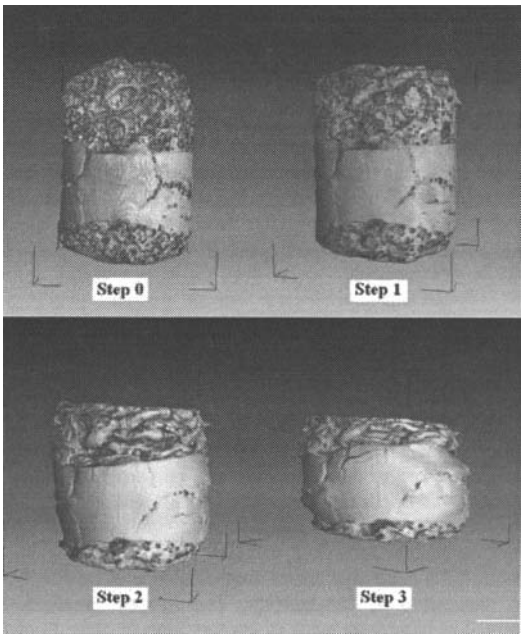

Fig. 3 Rendering of the reconstructed volume of the Al foam sample after each compression step.

The evolution of a representative sections of the samples during each compression step is showed in fig. 4.

At first deformation occurs only in the weakest zones of the samples (step 1), in particular in the upper part of the sample where drainage and coarsening during foaming are responsible for the thin cell walls and the big pore dimensions. Further compression leads to cells collapse and densification (steps 2 and 3) that progressively propagates in a wide region of the sample.

Results of the geometric evaluation of cells during compression are expressed through the equivalent diameter and circularity, calculated by means of equation (1) and (3) respectively.

Fig. 5 shows the histogram of the cells number according to the equivalent diameter values after each compression step. Fig. 6 shows the histogram of the cells number according to the circularity values after each compression step.

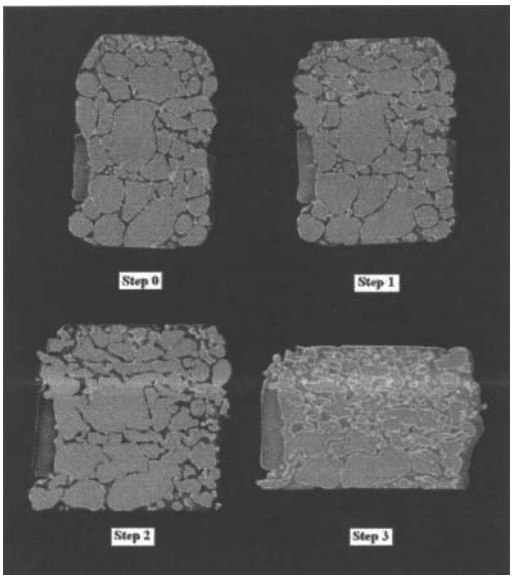

Fig. 4 Images of representative section of the Al foam sample after each compression step.

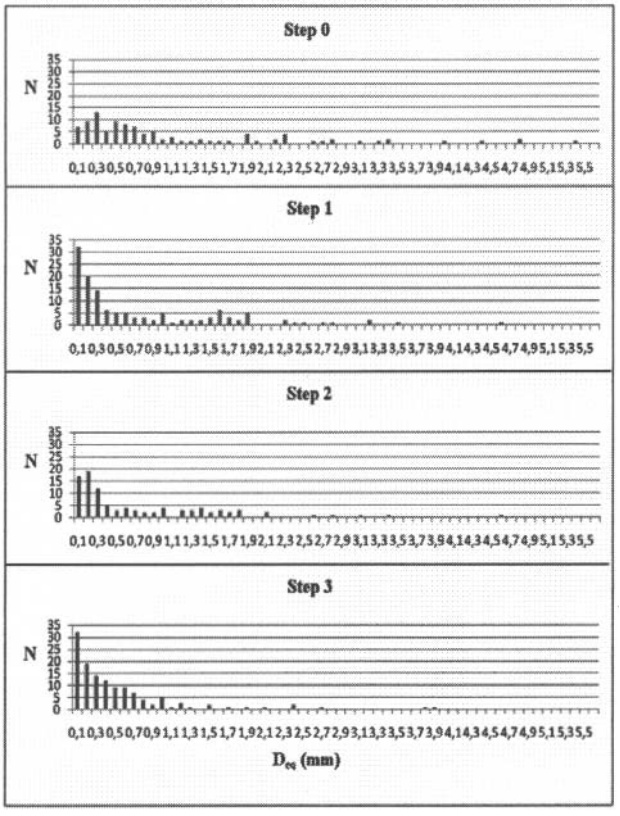

Fig. 5 Histogram of the cells number N vs. the equivalent diameter values D_{eq} (mm) after each compression step.

Going on compression, cells reduce progressively their dimensions: at each compression step it can be observed the disappearance of cells with the greatest equivalent diameter.
The number of cells with the smallest diameter increases from step 0 to step 1, decreases from step 1 to step 2 and increases again in the step 4, approaching the final collapse.
The circularity shows the same trend of the equivalent diameter: the number of cells with C=1 increases from step 0 to step 1 and from step 2 to step 3, allowing to deduce that the smallest cells have a close spherical shape.

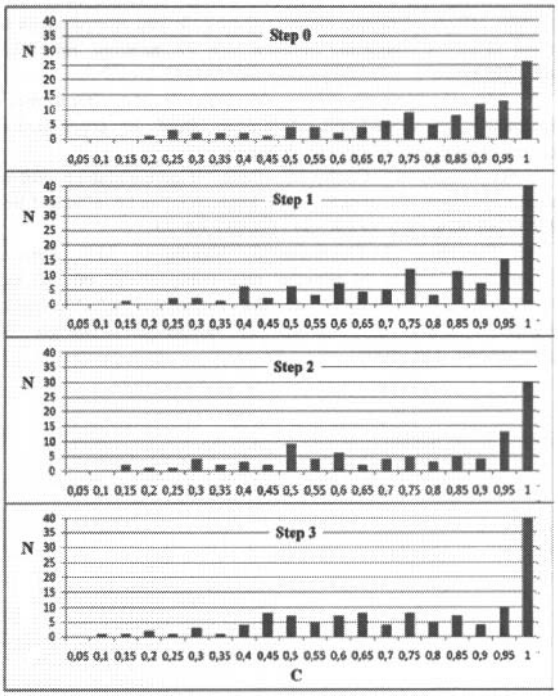

Fig. 6 Histogram of the cells number N vs. the values of circularity C after each compression step.

Conclusions

Compression tests were performed on the same sample of Al foam at increasing deformation steps with the aim to observe cells behaviour by X-ray computerized tomography. During compression steps at first deformation occurs in the weakest zones of the samples, leading to cells collapse and densification that progressively propagates in a wide region until their final densification. At each compression step it can be observed the disappearance of cells with the greatest equivalent diameter, until the reduction of the total cells number occurs at the final step. Cells morphology changes during compression: in particular the cells with the smallest diameter keep a shape close to spherical, also in the final compression step.

References

1. P.R. Onck, E.W. Andrews, L.J. Gibson, "Size effects in ductile cellular solids: Part I, Modeling", *International Journal of Mechanical Sciences*, 43 (2001), 681-699.

2. D.P. Papadopoulus, I.Chi. Konstantinidis, N. Papanastasious, S. Skolianos, D.N. Tsipas, "Mechanical properties of Al metal foams", *Material Letters*, 58 (2004), 2574-2578.
3. H. Yu, Z. Guo, Bing Li, G. Yao H. Luo, Y. Liu, "Research into the effect of cell diameter of aluminium foam on its compressive and energy absorption properties", *Material Science and Engineering A*, 454-455 (2007), 542-546.
4. F. Campana, D. Pillone, "Effect of wall microstructure and morphometric parameters on the crush behaviour of Al alloy foams", *Materials Science and Engineering A*, 479 (2008), 58-64.
5. H.W. Song, Q.J. He, J.J. Xie, A. Tobota, "Fracture mechanisms and size effects of brittle metallic foams: in situ compression test inside SEM", *Composites Science and Technology*, 68 (2008), 2441-2450.
6. Y. Mu, G. Yao, L. Liang, H. Luo, G. Zu, "Deformation mechanims of closed-cell aluminum foam in compression", *Scripta Materialia*, 63 (2010), 629-632.
7. Y.W. Kwon, R.E.Cooke, C. Park, "Representative unit-cell models for open-cell metal foams with or without elastic filler", *Mater. Sci. Eng. A – Struct.*, 343 (2003), 63-70.
8. G. Costanza, G. Gusmano, R. Montanari, M.E. Tata, N. Ucciardello, "Effect of powder mix composition on Al foam morphology", *Proceedings of the Institution of Mechanical Engineers, Part L: Journal of Materials: Design and Applications*, 222 (2008), 131-140.